DIAS: Differential Absorption of Sound to Obtain Temperature Profiles from Multifrequency Sodar

STUART BRADLEY

Physics Department, The University of Auckland, Auckland, New Zealand, and School of Acoustics and Electronic Engineering, University of Salford, Salford, United Kingdom

VICKY HIPKIN

Physics Department, The University of Auckland, Auckland, New Zealand

(Manuscript received 20 June 2001, in final form 14 November 2001)

ABSTRACT

The differential absorption of sound (DIAS) depends on frequency, temperature, and humidity in a known fashion. By obtaining turbulent reflections at two or more frequencies from the same target air mass, it is possible to resolve other frequency-dependent factors and obtain estimates of the absorption coefficient at the sounding frequencies. Over a restricted range of frequency and humidity, it is shown that the differential absorption is essentially a function of temperature but not of humidity. This method therefore provides the potential for temperature sounding using conventional sodars.

The theory of this method is outlined, and sensitivity is estimated based on actual sodar data. As part of the Tekapo Field Experiment in the Southern Alps, two sodars were operated side by side at a range of frequencies, allowing estimates to be made of signal-to-noise ratio. Temperature retrievals using this method are discussed.

1. Introduction

Differential absorption of light (DIAL) is an established method of using backscatter at two lidar wavelengths to sense trace gas concentrations. The wavelengths are chosen to lie outside and within an absorption band for the trace gas.

In the case of the differential absorption of sound (DIAS), the absorbing species are O_2, N_2, and H_2O. In the troposphere, the first two species are well-mixed, and H_2O is variable. Intuitively it might seem that the DIAL method could be extended to sound, with H_2O as a trace gas. However, absorption does vary also with temperature, with a dependence that varies with frequency. The dependence of absorption on humidity, temperature, and frequency is well known (Neff 1975). There is a strong motivation to obtain profiles of temperature and humidity using a sodar, since this would result in a single unit obtaining profiles of all the most important quantities (wind, turbulence, temperature, and moisture) for boundary layer characterization.

Clearly one approach would be to use several frequencies to try to solve nonlinear simultaneous equations for humidity and temperature. Gething and Jensen (1971) have taken this approach with four frequencies, but the dependence of absorption on humidity and temperature was not readily separable, and large errors were predicted. Brown and Hall (1978) tested the method on experimental data and also obtained errors of around 10 K. For sodar retrievals of temperature to be acceptable, errors should not be more than a few tenths of a degree. The difficulty with the Gething and Jensen method arises essentially from differencing four closely related measurements, and the lack of orthogonality in temperature, humidity, and frequency behavior.

In the present work we attempt to overcome these limitations by finding a form of the acoustic radar equation in which atmospheric variations are separated from frequency dependence. Then, by using water vapor *mixing ratio* rather than humidity (which is temperature-dependent), we isolate regions of parameter space that relate to temperature alone. This means that the set of equations to be solved is linear and explicit and not subject to the differencing and nonlinear approximation errors associated with previous methods.

Note that use of several frequencies is not generally a problem with sodar designs today. Current designs are invariably based on digitally controlled bandpass and low-pass filters.

The theoretical treatment below also gives a basis for

Corresponding author address: Stuart G. Bradley, School of Acoustics and Electronic Engineering, University of Salford, Salford M5 4WT, United Kingdom.
E-mail: s.g.bradley@salford.ac.uk

estimating the error in retrieved temperatures. A field experiment, in which two adjustable-frequency sodars were operated, allows temperature errors to be estimated and the prospect for efficient design of operational systems to be discussed.

2. Orthogonal form of radar equation

We write the sodar equation in the form

$$P = G\frac{\exp\left(-2\int_0^z \alpha\, dz\right)}{z^2}\chi, \tag{1}$$

where P is the received power, G includes the transmitted power and antenna factors, z is the range, α is the atmospheric absorption per unit length, and χ is the scattering cross section per unit volume and per unit solid angle. Taking logarithms,

$$Y(f, z) = f^n A(z) + S(z) + p(z)\ln f \tag{2}$$

where

$$Y = \ln\left(\frac{Pz^2}{G}\right), \tag{3a}$$

$$f^n A = -2\int_0^z \alpha\, dz, \quad \text{and} \tag{3b}$$

$$f^p e^S = \chi. \tag{3c}$$

This collects the observables into Y and separates the dependence of α and χ on frequency f from their atmospheric profile dependence. Simple power-law relations have been assumed for the frequency dependence; these will be tested below.

Parameter p is related to the slope of the temperature fluctuation spectrum. Parameter S includes information about strength of turbulence. Parameter A is of interest since it is temperature- and humidity-dependent and is related to the vertical profiles of these quantities. Since Y is known (from calibration and field measurements), and S represents a target that is the same for each interrogating frequency, it should be possible to estimate A.

Equation (2) is amenable to linear least squares regression to find parameters S, p, and A at each range z, given N measurements at a number of frequencies f, and provided n can be estimated:

$$\begin{pmatrix} N & \sum \ln f & \sum f^n \\ \sum \ln f & \sum [\ln f]^2 & \sum f^n \ln f \\ \sum f^n & \sum f^n \ln f & \sum f^{2n} \end{pmatrix}\begin{pmatrix} S \\ p \\ A \end{pmatrix} = \begin{pmatrix} \sum Y \\ \sum Y \ln f \\ \sum Y f_n \end{pmatrix}. \tag{4}$$

Parameter A is a measure of integrated absorption from the surface to the range z, and may be approximated by

$$A_J \approx -2f^{-n}\sum_{j=1}^{J} \alpha_j(z_{j+1} - z_j) \quad \text{or} \tag{5a}$$

$$\alpha_{j+1} \approx -\frac{A_{j+1} - A_j}{z_{j+1} - z_j}\frac{f^n}{2}. \tag{5b}$$

Each α_j can then be related to the temperature and humidity in the layer z_{j-1} to z_j, giving an estimate of the absorption profile. More generally, this is an inverse problem that could be, with appropriate knowledge of covariances, treated as a constrained least squares solution (Rodgers 2000).

The absorption coefficient α is the sum of contributions from classical absorption (dependent on f^2), vibrational absorption from O_2 molecules (also dependent on f^2 in the range of frequencies of interest), and vibrational absorption from N_2 molecules (with dependence of f^2 to f^0 over the minisodar frequencies). The vibrational absorption is modified by the presence of water vapor and is temperature-dependent. The difficulty is that higher temperatures and moisture content give the same absorption of sound as lower temperatures and moisture content, so a potential ambiguity exists in determining either temperature or moisture uniquely from atmospheric absorption measurements. Note that other loss mechanisms are small. For example, the scattering coefficient from turbulent temperature fluctuations is typically a factor of 10^{-4} smaller than α.

Figure 1 shows the variation of α with water vapor mixing ratio w and temperature T at a pressure of 1013 hPa and at $f = 2.5$ kHz and 5.0 kHz. The striking feature of these plots is the decoupling from temperature at a low mixing ratio and decoupling from mixing ratio in more moist regimes. In practice, most situations (except for desert or polar cases) fall into the latter category, and α is essentially independent of mixing ratio. The region where mixing ratio dependence gives way to temperature dependence can be estimated by the slope of the contour lines shown in Fig. 1. We find the critical w value where

$$\frac{\partial\alpha}{\partial w}\Delta w = \frac{\partial\alpha}{\partial T}\Delta T \tag{6}$$

for $\Delta w = 1$ g kg^{-1} and $\Delta T = 1$°C (corresponding to 45° slope in the above plots). This critical value varies from 8 to 11 g kg^{-1} as frequency varies from 2.5 to 5 kHz. It should be possible to resolve the temperature–moisture ambiguity further by including surface measurements made with other instruments.

3. Error estimation for T

In the region where α is a function of f and T (and only weakly dependent on w) we find the best fit to n from Eq. (3b) in the form

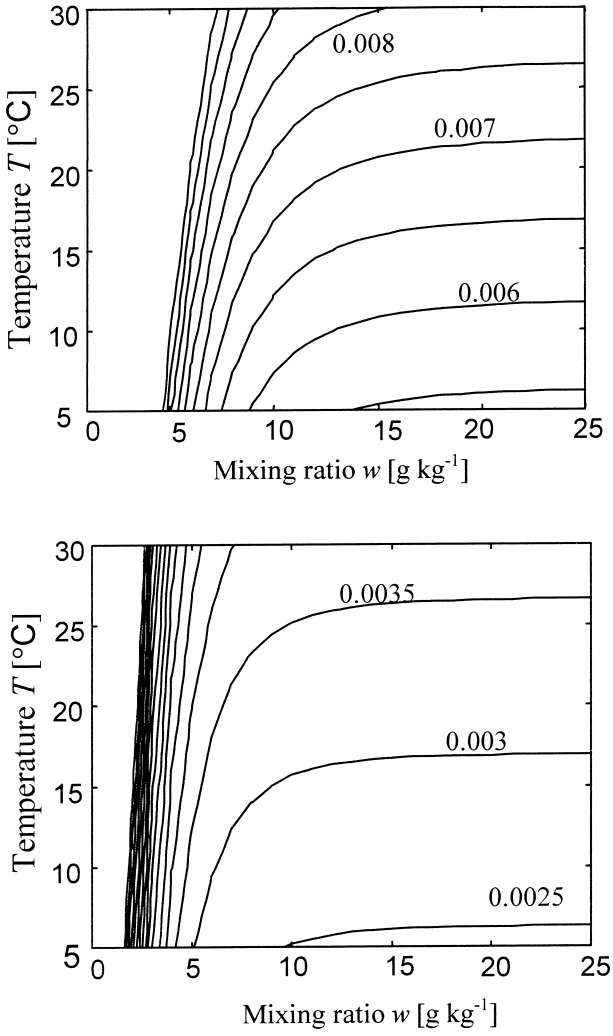

FIG. 1. Contours of linear absorption coefficient α (m^{-1}) at frequency (top) 5 kHz and (bottom) 2.5 kHz.

$$\ln\alpha = n \ln f + \ln\left(-\frac{1}{2}\frac{dA}{dz}\right). \tag{7}$$

This results is a very slight T dependence for n, varying from $n = 1.14$ at 5°C to $n = 1.10$ at 30°C.

Assuming $n = 1.12$, A is now found to be nearly linear in T and essentially independent of f. The error in temperature is shown in Fig. 2, when it is assumed $n = 1.12$ and when fitting with a simple straight line.

If a Kolmogorov spectrum is assumed, then p is fixed and we write

$$\mathbf{Y}^* = Y - p \ln f = \mathbf{S} + f^n\mathbf{A} \tag{8}$$

so that

$$\mathbf{A} = \frac{N\sum Y^* f^n - \sum Y^* \sum f^n}{N\sum f^{2n} - \left(\sum f^n\right)^2}. \tag{9}$$

Physically this means that knowledge of the sodar

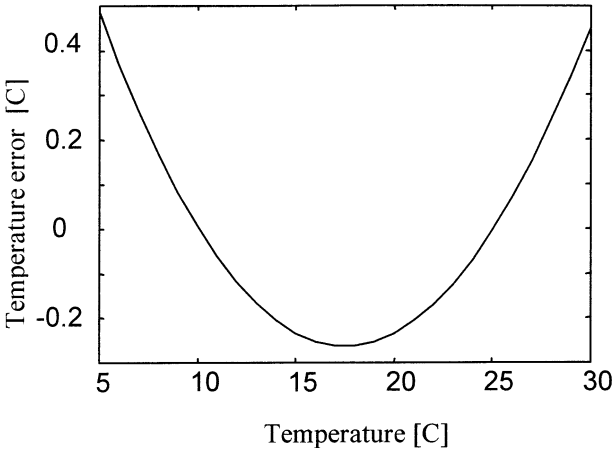

FIG. 2. Error in temperatures based on $n = 1.12$ and a linear relationship with A.

parameters together with the measurements of received power at several frequencies give a matrix $\mathbf{Y}^*$. Matrix $\mathbf{S}$ is related to the turbulent structure of the atmosphere and matrix $\mathbf{A}$ is related to the absorbing properties of the atmosphere. If the variance in all $\mathbf{Y}^*$ measurements is the same, then the error in estimates of $\mathbf{A}$ will be

$$\sigma^2_{\mathbf{A}} = \frac{N}{N\sum f^{2n} - \left(\sum f^n\right)^2}\sigma^2_{\mathbf{Y}^*}. \tag{10}$$

If only two frequencies, f_1 and f_2, are used, then from (2), (8), and (10)

$$\sigma^2_T = \frac{1}{N(f_1^n - f_2^n)^2}\left(\frac{\sigma^2_P}{P^2} + \frac{\sigma^2_p}{[\ln f]^2}\right)\left(\frac{\partial T}{\partial \mathbf{A}}\right)^2, \tag{11}$$

where fluctuations in p have also been allowed for.

The question is whether we can detect the temperature-related changes in α, which, as shown in Fig. 1, are around 1% deg^{-1}. A field experiment was conducted in which two AeroVironment sodars having the characteristics given in Table 1 were used. The field situation was on uniform flat terrain in the Lake Tekapo valley in the Southern Alps of New Zealand. Measurements were conducted during the night under stable conditions. The two sodars ran independently, with a separation of 30 m. Each could have the transmitting frequency adjusted in 100-Hz increments. The low-frequency sodar speakers and enclosure became inefficient above 3 kHz, and the high-frequency sodar was inefficient below 3 kHz. Typical power levels and variations for nighttime conditions at Tekapo are shown in Fig. 3, where both

TABLE 1. Sodar properties.

Model	Default frequency (Hz)	Frequency range (Hz)	Nominal height range (m)
3000	2800	2500–3300	500
4000	4500	4400–6000	200

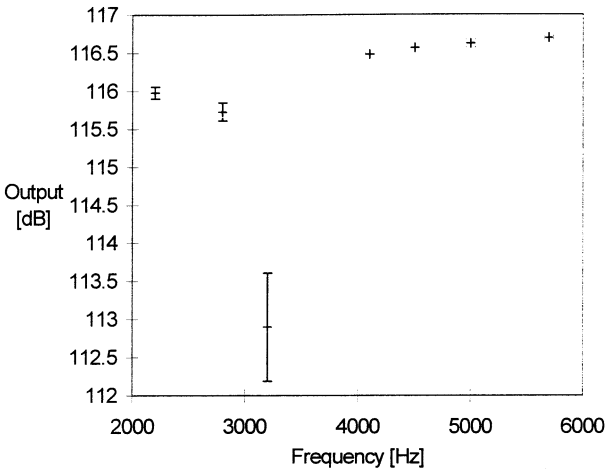

FIG. 3. Received power (arbitrary dB origin) from the two sodars. Error bars are shown for 1 std dev.

sodars give decreased power received at 3 kHz, with corresponding higher variance in the signal.

From this Fig. 3, $\sigma_P/P \sim 0.02$ except for the region around 3 kHz, and from the absorption regressions $\partial T/\partial A = 1.3 \times 10^8$ °C $\text{Hz}^{1.12}$ and with half-hour averaging, the σ_T values in Table 2 are obtained, assuming fixed p. If the two sodars are operated at their design frequencies, the standard deviation in temperature estimates is predicted to be 0.7 K. If the Model 4000 sodar is operated at the two extremes of its useful frequency range, a similar error is predicted. The best performance predicted for this particular combination of sodars is 0.3 K, which is sufficiently low to be of practical use.

Note that these data are derived from raw signal returns. In practice, all sodars employ consistency checks over height and time, and such constraining/smoothing methods would be expected to reduce temperature profile uncertainty.

4. Discussion

This investigation indicates that the orthogonalization of the sodar equation, together with judicious separation of variables, can potentially allow useful temperature retrievals. Ideally a sodar designed for this task would be capable of transmitting at two or more widely separated frequencies. This is currently unusual in commercial sodars, but given the wide band performance of speakers, there is no fundamental reason why such a sodar cannot be designed. Careful thought would need to be applied though to beam forming, since the beamwidth is a function of frequency, and there is an inherent assumption in this method that the same turbulent volume is being sampled at each frequency. However, the field experiment described above had beams separated in space by around 30 m.

We have evaluated errors for only the two-frequency case. If more frequencies are used, the errors will decrease, but probably only as the root of the number of frequencies (if their separation is the same); this suggests that perhaps three frequencies would be worthwhile.

TABLE 2. Temperature errors σ_T (°C) for different frequency pairs.

Frequency (Hz)	2800	3200	4100	4500	5000	5700
2200	1.9	1.2	0.6	0.5	0.4	0.3
2800		2.8	0.9	0.7	0.5	0.4
3200			1.2	0.8	0.6	0.4
4100				2.7	1.2	0.7
4500					2.2	0.9
5000						1.5

Systematic error in temperature retrieval arises from the assumptions made, whereas random errors arise from random measurement noise. These systematic errors can be reduced by including other independent measurements in the dataset. For example, surface measurements of T could be used to optimize the choice of n and hence locate the minimum received power of Fig. 3 optimally for the current environment.

One assumption made is that p is fixed at 1/3 (the Kolmogorov spectrum assumption). For the error in p to contribute as much error as P, σ_p would need to be about 50% of the Kolmogorov value, that is, fluctuations in the range $0.3 < p < 0.37$. These are quite large fluctuations and, if commonly occurring, would call into question the whole quantitative use of sodars.

The sodars used in this study report received power and Doppler spectra at 5-m intervals vertically, although adjacent measurements are not independent. It is not necessary, in most situations, to obtain temperature profiles to this resolution. The most likely improvement in temperature retrieval accuracy is therefore likely to arise from obtaining temperatures at a reduced number of heights. Ongoing research extends this work and the results of Bradley and Hipkin (2000) to include constrained inversion of the orthogonal sodar equations to optimize the temperature retrieval model.

Acknowledgments. The authors are grateful for use of a sodar from AeroVironment, and for help in the field by Andy Sturman's team from the University of Canterbury, and University of Auckland coworker Tracey Webb.

REFERENCES

Bradley, S. G., and V. J. Hipkin, 2000: DIAS: Differential absorption of sound to obtain temperature profiles from multi-frequency SODAR. *Proc. 10th Int. Symp. on Acoustic Remote Sensing,* Auckland, New Zealand, ISARS, 111–114.

Brown, E. H., and F. F. Hall, 1978: Advances in atmospheric acoustics. *Rev. Geophys. Space Phys.,* **16,** 47–110.

Gething, J. T., and D. Jensen, 1971: Measurement of temperature and humidity by acoustic echo sounding. *Nat. Phys. Sci.,* **231,** 198–200.

Neff, W. D., 1975: Quantitative evaluation of acoustic echoes from the planetary boundary layer. NOAA Tech. Rep. ERL 322-WPL 38, 34 pp.

Rodgers, C. D., 2000: *Inversion Methods for Atmospheric Sounding. Theory and Practice.* Series on Atmospheric, Oceanic and Planetary Physics, Vol. 2, World Scientific, 256 pp.